



Establishment of generic transformations for geotechnical design parameters

Jianye Ching^{a,*}, Kok-Kwang Phoon^b

^a Dept. of Civil Engineering, National Taiwan University, Taipei, Taiwan

^b Dept. of Civil and Environmental Engineering, National University of Singapore, Singapore

ARTICLE INFO

Article history:

Received 15 August 2011

Received in revised form 12 December 2011

Accepted 12 December 2011

Available online 8 January 2012

Keywords:

Transformation uncertainty
Geotechnical design parameter
Reliability-based design
Correlation
CPTU tests
Undrained shear strength

ABSTRACT

Geotechnical design parameters are typically estimated based on the transformations from site investigation results. In general, one expects the transformation uncertainty to change depending on the number and type of sites in the database. This study tries to address the following two issues pertaining to the transformation uncertainty: (a) how transformation uncertainties change with the number and type of sites in the database and (b) whether transformation uncertainties will eventually fall within a narrow range when a “generic” transformation is developed from a sufficiently large database. This study also attempts to propose a framework to establish such a generic transformation and quantify its uncertainty. This framework is demonstrated by the transformation between piezocone CPTU data and undrained shear strengths (S_u) of clays. It was found that the CPTU– S_u transformation and its uncertainty is site or region-dependent, and the “local” transformation equation from one site may not be applicable to another site, both in terms of the mean trend (which is well known) as well as the coefficient of variation (c.o.v.). An approach is proposed to develop the generic CPTU– S_u transformation equations that can be applied for downstream reliability analysis or design in the absence of local data. Sensitivity analysis shows that it requires data from at least 15 sites with the accompanying implicit assumption that sufficient geographical coverage typically implies sufficient geologic diversity to reliably build such “generic” transformation equations.

© 2011 Elsevier Ltd. All rights reserved.

1. Introduction

Geotechnical designs require careful assessment for the mean values and variabilities of design parameters such as soil shear strength and modulus. These design parameters are typically estimated based on transformations from site investigation results. Quantification of transformation uncertainty [1,2] is essential when reliability analysis and reliability-based design are of concern. In the case where local experiences are sufficient, the mean value and coefficient of variation (c.o.v.) of a design parameter can be readily identified. As a real example, empirical data between undrained shear strength (S_u) and SPT – N value from 25 sites in Japan indicate that [3]

$$\log_{10}(S_u/P_a) = 0.72 \times \log_{10}(N) + \log_{10}(0.29) + \varepsilon \quad (1)$$

where P_a is atmosphere pressure, and ε quantifies the transformation uncertainty for this S_u – N transformation: it has zero mean and standard deviation equal to 0.15 [2]. Given the site investigation result for SPT – N value, the mean value and c.o.v. of S_u can be readily identified.

It is reasonable to question whether or not the mean trend and its uncertainty given in (1) can apply to a site outside Japan, given

that N may not be only affected by S_u (e.g., stress history, plasticity index, and sensitivity may also affect N). There can be two major concerns: (a) whether the mean trend can be extrapolated to a site outside Japan and (b) whether the standard deviation of 0.15 can be extrapolated to that site. The above concerns are valid because the clay at the site may not have the same stress history, plasticity index, and sensitivity as the Japan clays. For the first question, the mean trend based on Japan data, in principle, should not be extrapolated to a site outside Japan. In fact, such extrapolation may not be necessary because the local mean trend for the site can be reliably estimated based on site investigation data derived from this site. The second question is rather important for reliability-based design (RBD). For this question, however, site investigation data derived from a single site are typically insufficient to characterize the transformation uncertainty. As a result, it is desirable to know whether this 0.15 standard deviation based on Japan experiences is “generic” so that the extrapolation to a site outside Japan is reliable.

The present paper focuses on the transformation uncertainty (second-order statistics) and this must be clearly distinguished from the better known mean trend (first-order statistics). The mean trend is loosely called the “regression equation” in the literature and it is occasionally reported without the data scatter. In principle, one expects the transformation uncertainty to change depending on the number and type of sites in the database. To our knowledge, no one really knows: (a) if transformation

* Corresponding author. Tel.: +886 2 33664328.

E-mail address: jyching@gmail.com (J. Ching).

uncertainties are comparable or to what degree are they incomparable given the unavoidable differences in the underlying local databases and (b) if transformation uncertainties will eventually fall within a narrow range when a generic transformation is developed from a sufficiently large database. As mentioned above, the first question is rather important for RBD, particularly in situations where there are sufficient local data to estimate the mean trend but insufficient to characterize the uncertainty. It is reasonable to assume that a generic correlation trend will produce a large “generic” transformation uncertainty that can be conservatively applied to sites where relevant local data are insufficient. Under this assumption, we would need to have a means for estimating this “generic” transformation uncertainty.

The main objective of this study is to examine the above issues pertaining to local versus generic transformation uncertainties. As a demonstration, the transformation between cone resistance in a piezocone test (CPTU) and S_u is studied. In particular, local CPTU– S_u trends and magnitudes of the local transformation uncertainties will be studied to verify if the above issues are of practical significance. An approach will be proposed to estimate the magnitudes of the generic transformation uncertainties based on a generic CPTU– S_u database. A procedure of verifying whether the obtained transformation equation is indeed generic is proposed and demonstrated. The practical outcomes of this study consist of simplified formulas for estimating the mean values and coefficients of variation (c.o.v.) of S_u based on the CPTU results. These formulas are expected to work well even for cases where local data are not available. This paper does not seek to improve existing CPTU– S_u correlation equations or to propose new ones, but seek to clarify the uncertainties underlying these correlations (usually mean trends) based on available data in the literature. In short, the focus is not on the well known regression line, but the data scatter about this line. A systematic study of the behavior of this data scatter under different regression scenarios (“local” single site or “generic” multiple worldwide sites) is particularly useful for RBD.

2. CPTU– S_u transformations

The CPTU test is increasingly popular nowadays for profiling S_u because it is quick, relatively reliable and potentially able to construct continuous profiles [4–9]. Previous studies [4–6,9–33] typically compiled data points for some local regions (e.g. Hong Kong, Vancouver, London, etc.) to develop the CPTU– S_u transformation equations. A more sophisticated study involving estimating of S_u from multivariate data such as CPTU, SPT, and OCR, was carried out recently [34]. To our knowledge, this study is the first of its kind to construct multivariate correlations (CPTU–SPT– S_u) from existing pairwise correlations (e.g., CPTU– S_u , SPT– S_u) within a rigorous Bayesian framework. However, [34] assumed that the transformation uncertainties associated with pairwise correlations can be readily estimated based on the data scatter. Although this is true, it is reasonable to question if the results can be applied to another site located in a different region, which was not addressed in [34].

There are at least three correlation models for S_u based on CPTU results [5,7]: (a) N_{KT} model; (b) N_{KE} model; and (c) $N_{\Delta u}$ model. These models propose non-dimensional parameters N_{KT} , N_{KE} and $N_{\Delta u}$:

$$N_{KT} = \frac{q_T - \sigma_{v0}}{S_u} \quad N_{KE} = \frac{q_T - u_2}{S_u} \quad N_{\Delta u} = \frac{u_2 - u_0}{S_u} \quad (2)$$

where $q_T = q_c + (1 - a)u_2$ is the corrected total cone resistance; q_c is the uncorrected cone resistance, u_2 is the pore pressure measured right behind the cone, and a is the area ratio of the cone; σ_{v0} is the total vertical stress; u_0 is the hydrostatic pore pressure. Let us employ the following unified notation:

$$N_j = \frac{\theta_j}{S_u} \quad (3)$$

where $N_1 = N_{KT}$, $N_2 = N_{KE}$ and $N_3 = N_{\Delta u}$, while $\theta_1 = q_T - \sigma_{v0}$, $\theta_2 = q_T - u_2$ and $\theta_3 = u_2 - u_0$. These cone “N factors” are found to be empirically correlated to the pore pressure ratio (B_q):

$$B_q = \frac{u_2 - u_0}{q_T - \sigma_{v0}} \quad (4)$$

In Lunne et al. [35] and Karlsrud et al. [36], the CPTU– S_u correlations are studied, and Fig. 1 summarizes the possible ranges of these N factors (the dashed red lines) proposed by these studies. Apart from these studies, Kulhawy et al. [37] examined a large database of CPTU– S_u correlations and summarized that N_{KT} is on average $1/0.0789 = 12.7$ with a c.o.v. of 0.35. In the following section, a global CPTU– S_u correlation database compiled from available data in existing literature will be presented, and these ranges and conclusions will be re-examined with greater rigor.

3. CPTU– S_u database

A global database of CPTU tests is compiled. There are in total 38 sites worldwide in the database, nearly 1/3 of the sites were mentioned in [38]. Table 1 summarizes the background information for the 38 sites. Among them, 13 sites in Canada, 8 sites near Norway (including North Sea), 5 sites are located in the United States, 3 sites in Brazil, 3 sites in Britain, 2 sites in Venezuela, 1 site in Hong Kong, and 1 site in Italy. The clays range from normally consolidated to medium over-consolidated clays; the clays of ten sites are sensitive with sensitivity up to 500.

All sites were tested with standard electric cones; four sites do not have the pore pressure information u_1 or u_2 . The area ratios a for the test cones ranges from 0.38 to 0.82. The data for each site is typically composed of the following items: (1) q_c profile; (2) u_2 profile; and (3) either the tested S_u values at selected depths (by laboratory UU, UC, CIUC, CAUC tests) or the S_u profile from field vane shear tests (VSTs). The number of data points listed in the table denotes the number of S_u data points for each site, ranging from 2 to 27 data points. The total number of data points is 482. Among the 38 sites, the Atterberg limits for 33 sites are known at selected depths, and OCRs are known for 33 sites at selected depths.

The original data points are pre-processed based on available information to ensure that subsequent analyses would be as consistent as practically possible:

1. All q_c are converted into q_T to correct for the effect of pore pressure generated behind the cone. This requires the knowledge of u_2 and area ratio a . There are 15 sites, where a is not documented. For these cases, an average a value = 0.7 is assumed, because a typically ranges from 0.55 to 0.9 [41] and because 0.7 is also the average a value for our database. There are also four sites, where the pore pressure is not measured. For these cases, the correlation equations suggested by Mayne et al. [42] is adopted to estimate u_2 based on q_c .
2. All measured pore pressures are converted into u_2 . There are seven sites where u_1 (pore pressure at cone tip) rather than u_2 is measured. In this case, the correlation equation suggested by Mayne et al. [42] is used to convert u_1 into u_2 .
3. The vertical total stress is estimated from the soil profile. In the cases where the soil unit weights and water table depths are not known, reasonable estimates are made. Note that bulk unit weight of soil varies over a relatively narrow range and water table depth affects it marginally due to saturation. Hence, it is possible to obtain reasonable estimates of the vertical total stress even in the absence of bulk unit weights and water table depths.

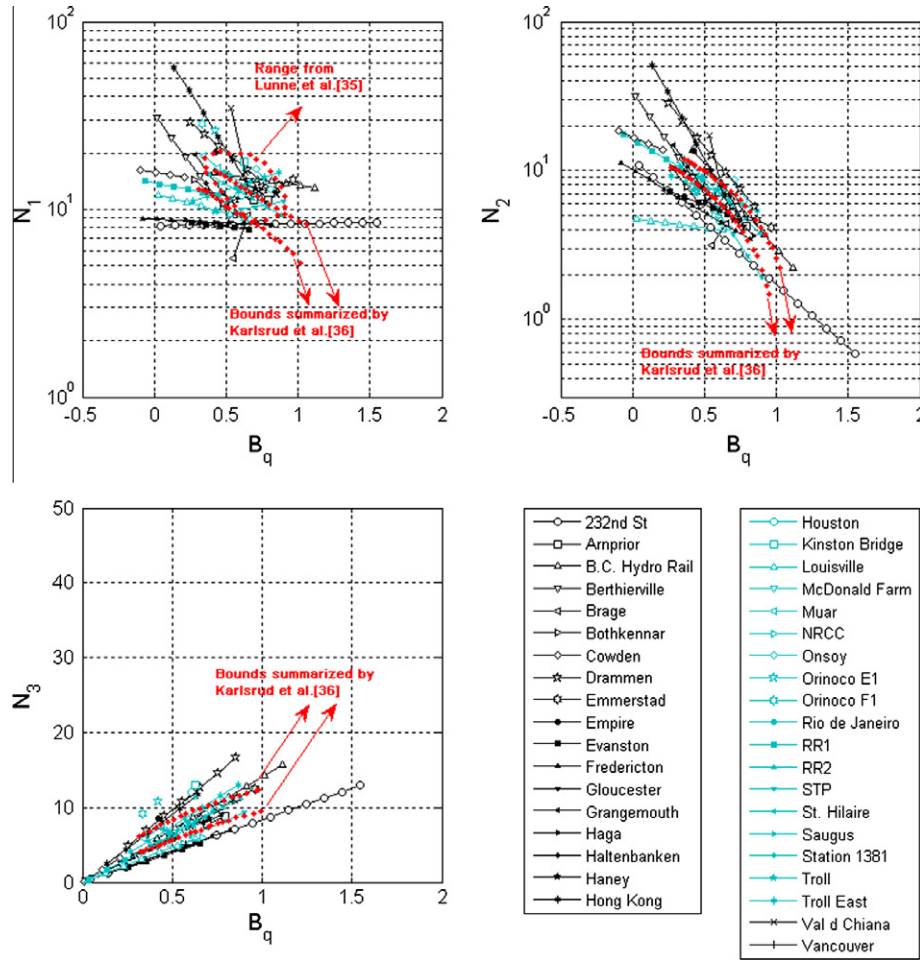


Fig. 1. Proposed bounds and ranges for N_1 , N_2 and N_3 reported in the literature and the local correlation trends.

4. All measured S_u is converted into the equivalent CIUC values: CAUC to CIUC based on [43], UU and UC to CIUC based on [44], and VST to field value based on [45] (see Table 2). Note that the field value is similar to a DSS value. These DSS values are further converted to CIUC values using the transformation equations suggested by Kulhawy and Mayne [43].

Ideally, only data sources with complete documentation should be used. Nonetheless, perfect data sources are rare and all current statistical characterization studies in the literature involve making appropriate assumptions to ensure that the sample size is large enough to produce reasonably robust statistics such as coefficients of variation. The appropriateness of these assumptions would be validated using an independent database in the last section of this paper.

The (local) mean values and c.o.v.s of N_1 , N_2 and N_3 for each site are calculated. The local average values of N_1 range from 8.50 (232nd Street) to 27.48 (Orinoco F1) with overall average of 14.74; the overall average agrees well with the conclusion of [37]. The broad range of the local average values indicates that the experience from one site may not be applicable to another site. This observation is already widely known. The c.o.v.s of N_1 range from 0.04 (Orinoco E1) to 0.76 (Berthierville). Note that this c.o.v. not only includes local transformation uncertainties but also includes measurement errors in q_T and S_u and probably the transformation uncertainties in Table 2. At this moment, it is not possible to isolate the local transformation uncertainty from this “lumped” uncertainty. Similar observations are found for the local average values and c.o.v.s for N_2 and N_3 except that the ranges are different.

In summary, the local mean values and c.o.v.s demonstrates quite convincingly that both average and c.o.v. values for the cone factors are strongly site dependent.

Fig. 1 further shows the mean correlations for N_1 , N_2 , N_3 versus B_q for selected regions – these are in general the local trends for the correlations. In addition, “bounds” given in the literature are shown for comparison. The following observation is clear: the so-called “bounds” summarized by available literature can be exceeded by the local trends. A practical corollary is that the “bounds” may not be suitable for all sites in the database. The reported “bounds” in the literature appear to be local in the sense of being site dependent, rather than genuine generic bounds applicable to all sites, e.g. the bounds for Lunne et al. [35] are derived only based on data in North Sea. This study focuses only on the effect of B_q on N_1 , N_2 , N_3 , because this information is commonly available in the global database and reasonable correlations were found. A reasonable correlation is needed to make it worthwhile to consider an additional piece of information such as B_q , because it can reduce transformation uncertainty. Another commonly available field in the database is the plasticity index, but the correlations between N_1 , N_2 , N_3 and the plasticity index were found to be weak (not shown).

Fig. 2 shows all data points of all sites for the three models. It is clear that a linear correlation seems reasonable for $\ln(N_1)$ versus B_q , $\ln(N_2)$ versus B_q and N_3 versus B_q relationships. Therefore, the following correlation models are adopted in the ensuing analysis:

$$\ln(N_1) \approx a_1 + b_1 B_q \quad \ln(N_2) \approx a_2 + b_2 B_q \quad N_3 \approx b_3 B_q \quad (5)$$

Note that $a_3 = 0$ follows from the definitions of N_3 and B_q .

Table 1

Basic information of the CPTU global database.

<i>k</i>	Site	Region	Clay description (range of sensitivity if available)	# Points with S_u	Area ratio	Filter location	S_u Test type					Atterberg limits	OCR	References
							UC	UU	CIUC	CAUC	VST			
1	232nd St.	Vancouver (Canada)	MOC silty clay (2–19)	21	0.8	u_2					*	–	–	[5,12,13]
2	Arnprior	Ottawa (Canada)	LOC sensitive gray	22	0.66	u_2			*		*	*	*	[6,14]
3	B.C. Hydro Rail	Vancouver (Canada)	LOC (7–10)	26	–	–					*	–	–	[5]
4	Berthierville	Quebec (Canada)	NC silty gray clay	10	0.82	u_2					*	*	*	[15]
5	Brage	North Sea	LOC silty clay	3	–	u_1				*		*	*	[11]
6	Bothkennar	Scotland (UK)	Silty clay	27	–	u_2		*			*	*	*	[39]
7	Cowden	Yorkshire (UK)	LOC blue–gray glacial	5	–	u_2				*		*	*	[11]
8	Drammen	Norway	NC lean marine/plastic clay (3–7)	25	0.78	u_2				*	*	*	*	[9,11]
9	Emmerstad	Norway	MOC quick silty clay (>60)	4	0.38	u_2				*		*	*	[11]
10	Empire	Louisiana (USA)	NC silty gray clay	17	–	u_1	*	*				–	*	[16]
11	Evanston	Illinois (USA)	NC lean clay (1–3)	18	0.7	u_1		*			*	*	*	[17]
12	Fredericton	New Brunswick (Canada)	–	8	0.66	u_2					*	*	*	[6,18]
13	Gloucester	Ottawa (Canada)	LOC sensitive clay (100)	18	0.66	u_2			*		*	*	*	[6]
14	Grangemouth	UK	LOC dark gray clay	13	0.8	u_2	*					*	*	[19,20]
15	Haga	Norway	MOC lean gray clay	5	–	u_2				*		*	*	[11]
16	Haltenbanken	Norway	LOC silty sandy clay	3	–	u_2				*		*	*	[11]
17	Haney	Vancouver (Canada)	MOC (3–13)	27	–	–					*	–	–	[5]
18	Hong Kong	Hong Kong	MOC sensitive marine (4–7)	27	0.7	u_1					*	*	*	[10]
19	Houston	Houston (USA)	MOC light gray clay	4	–	–					*	*	*	[21]
20	Kinston Bridge	London	London clay	6	0.75	u_2					*	*	*	[22]
21	Louiseville	Quebec (Canada)	LOC gray silty/sensitive/organic clay (13–29)	14	0.82	–					*	*	*	[15]
22	McDonald's Farm	Vancouver (Canada)	NC gray clayey silt (2–7)	4	0.8	u_2					*	–	–	[6,12]
23	Muar	Malaysian Peninsula (Malaysia)	Marine clay	13		u_2					*	*	*	[23]
24	NRCC	Quebec (Canada)	MOC sensitive marine (10–500)	5	0.66	u_2					*	*	*	[6,24]
25	Onsoy	Norway	LOC sensitive marine (5–7)	5	0.8	u_2				*	*	*	*	[11]
26	Orinoco E1	Orinoco Delta (Venezuela)	CH–OH clay	5	0.7–	u_2					*	*	*	[25]
27	Orinoco F1	Orinoco Delta (Venezuela)	CH–OH clay	5	0.7	u_2					*	*	*	[25]
28	Rio de Janeiro	Brazil	MOC gray plastic clay (4)	11	0.75	u_2				*	*	*	*	[11,25,27,28]
29	RR1	Recife city (Brazil)	LOC organic clay (6–13)	17	–	u_1		*	*		*	*	*	[29]
30	RR2	Recife city (Brazil)	LOC organic clay (6–11)	14	–	u_2		*	*		*	*	*	[29]
31	STP	Ottawa (Canada)	MOC gray marine (40–500)	11	0.66	u_2		*			*	*	*	[6]
32	St. Hilaire	Montreal (Canada)	Weathered brown clay	10	0.7	u_2					*	*	*	[30]
33	Saugus	Massachusetts (USA)	Boston blue clay	15	0.7	u_2			*		*	*	*	[31]
34	Station 1381	Atchafalaya Basin, Louisiana (USA)	Highly plastic CH Clay	20	0.7–	u_2			*		*	–	*	[31]
35	Troll	North Sea	LOC gray plastic clay	5	–	u_1				*		*	*	[11]
36	Troll East	Norway	LOC plastic/lean sandy clay	23	–	u_2				*	*	*	*	[4]
37	Val d Chiana	Italy	MOC soft clay	14	–	u_1		*			*	*	*	[33]
38	Vancouver	Vancouver (Canada)	LOC clayey silt (3–5)	2	–	u_2				*		*	*	[11]

Notes: NC – normally consolidated ($1 \leq \text{OCR} \leq 1.3$); LOC – lightly over-consolidated ($1.3 < \text{OCR} \leq 3.0$); and MOC – medium over-consolidated ($3.0 < \text{OCR} \leq 10.0$) (definition of NC, LOC and MOC follows [40]).

Asterisk “*” means information is available.

4. Transformation uncertainties

Uncertainties can be classified into three categories: (a) inherent (spatial) variabilities of soil properties; (b) measurement errors during tests; and (c) transformation uncertainties in correlation models. The purpose of this study is to examine the magnitudes of the transformation uncertainties for the CPTU– S_u correlation models. It is therefore important to isolate the transformation uncertainties from the data scatter whenever it is practical to do so. In general, this data scatter is the combined outcome of the three aforementioned sources of uncertainties. Spatial variabilities can be minimized if the data is pre-processed carefully – the locations of the S_u and CPTU data used to calculate the N factors are fairly close in space (typically within a vertical interval of less than 0.3 m). Measurement errors cannot be easily removed.

Strictly speaking, the transformation uncertainties are the uncertainties that occur in the correlation between the “actual” values of soil parameters, rather than between the “measured” values of soil parameters. Using the CPTU– S_u correlations as an

example, if E_j denotes the transformation uncertainties for the N_j model, it is proposed that the “local” transformation is

$$\begin{aligned}
 \ln(N_1^{(k,i)}) &= \ln(\theta_1^{(k,i)} / S_u^{(k,i)}) = a_1^{(k)} + b_1^{(k)} B_q^{(k,i)} + E_{L,1}^{(k,i)} \\
 \ln(N_2^{(k,i)}) &= \ln(\theta_2^{(k,i)} / S_u^{(k,i)}) = a_2^{(k)} + b_2^{(k)} B_q^{(k,i)} + E_{L,2}^{(k,i)} \\
 N_3^{(k,i)} &= \theta_3^{(k,i)} / S_u^{(k,i)} = b_3^{(k)} \cdot B_q^{(k,i)} \cdot \exp[E_{L,3}^{(k,i)}]
 \end{aligned} \quad (6)$$

where the superscript “ k ” is the site index; the superscript “ i ” is the sample index; and the subscript “ L ” is to highlight that the transformation uncertainties are local. For instance, $B_q^{(k,i)}$ denotes the “actual” B_q value of the i th soil sample at the k th site, and the same notation applies to $E_{L,j}^{(k,i)}$ and $N_j^{(k,i)}$ – they are not the measured values but the actual values. Note that the transformation uncertainties for $\ln(N_1)$ versus B_q and $\ln(N_2)$ versus B_q are assumed to be additive based on the relatively constant data scatter in Fig. 2. On the other hand, the transformation uncertainty for N_3 versus B_q is multiplicative, because data scatter is clearly increasing with B_q . A detailed analysis based on model selection (AIC proposed by Akaike [46])

Table 2

Equations used for the conversion of undrained shear strength to equivalent CIUC values.

Test type	Equation	Reference
UU	$S_u(\text{CIUC}) \approx 0.243\sigma'_v + 0.821S_u(\text{UU})$	Chen and Kulhawy [44]
UC	$S_u(\text{CIUC}) \approx 0.237\sigma'_v + 0.853S_u(\text{UC})$	
VST	$S_u(\text{DSS}) \approx S_u(\text{field}) \approx \lambda \cdot S_u(\text{VST});$ λ depends on PI	Bjerrum [45]
	$S_u(\text{CIUC}) \approx [S_u(\text{DSS})]/(0.77 - 0.0064\phi')/$ $\text{OCR}^{0.776}/\text{OCR}^{0.709}$	Kulhawy and Mayne [43]
CAUC	$S_u(\text{CIUC}) \approx [S_u(\text{CAUC})]/(1.13 - 0.0094\phi')/$ $\text{OCR}^{0.738}/\text{OCR}^{0.709}$	Kulhawy and Mayne [43]

Notes: UU – unconsolidated undrained test; UC – unconfined compression test; VST – vane shear test; CIUC – isotropically consolidated undrained test; CAUC – anisotropically consolidated undrained test.

and BIC proposed by Schwarz [47]) clearly shows that an additive transformation uncertainty model is much less compatible to the $B_q - N_3$ data points.

For simplicity, the local transformation uncertainties for the N_j model within the k th site, i.e. $\{E_{L,j}^{(k,i)} : i = 1, \dots, n_k\}$ (n_k is the number of data points in the k th site) are assumed to be normally distributed with zero mean and standard deviation $\sigma_j^{(k)}$. Note that E_j contains purely transformation uncertainties with no measurement errors, so $\sigma_j^{(k)}$ purely quantifies transformation uncertainties. Observing that $B_q = \theta_1/\theta_3$, the third equation for the N_3 model in (6) can be reduced to

$$\ln(\theta_1^{(k,i)}) = \ln(b_3^{(k)}) + \ln(S_u^{(k,i)}) + E_{L,3}^{(k,i)} \quad (7)$$

The “generic” transformations are defined in an analogous way:

$$\begin{aligned} \ln(N_1^{(k,i)}) &= \ln(\theta_1^{(k,i)}/S_u^{(k,i)}) = a_1 + b_1 B_q^{(k,i)} + E_{G,1}^{(k,i)} \\ \ln(N_2^{(k,i)}) &= \ln(\theta_2^{(k,i)}/S_u^{(k,i)}) = a_2 + b_2 B_q^{(k,i)} + E_{G,2}^{(k,i)} \\ N_3^{(k,i)} &= \theta_3^{(k,i)}/S_u^{(k,i)} = b_3 \cdot B_q^{(k,i)} \cdot \exp[E_{G,3}^{(k,i)}] \end{aligned} \quad (8)$$

where the standard deviation of $E_{G,j}^{(k,i)}$ is σ_j ; the subscript G is to highlight that the transformation uncertainties are generic. Note that the superscripted k indices in a_j , b_j and σ_j are dropped because they are generic and not site-dependent.

We have noted previously that the scatter of the observed values is potentially augmented by measurement errors. Let us further denote the measured value of B_q by $\hat{B}_q^{(k,i)}$ and denote that of N_j by $\hat{N}_j^{(k,i)} = \hat{\theta}_j^{(k,i)}/\hat{S}_u^{(k,i)}$, where $\hat{S}_u^{(k,i)}$ and $\hat{\theta}_j^{(k,i)}$ are the “measured” undrained shear strength and CPTU data. According to [2], the c.o.v. of the measurement errors for S_u is on average 0.2 (ranging from 0.05 to 0.38) and that for the q_T is on average 0.1 (ranging from 0.05 to 0.15). The magnitude of the measurement error of B_q is unknown, but its standard deviation is herein estimated to be in the order of 0.1. These assumptions lead to the following expressions for the measured values of various soil parameters: for S_u

$$\hat{S}_u^{(k,i)} = D_{Su}^{(k,i)} \cdot S_u^{(k,i)} \quad (9)$$

where $D_{Su}^{(k,i)}$ is lognormally distributed with median value = 1 and c.o.v. = $\delta_{Su} \approx 0.2$; for the CPTU data

$$\hat{\theta}_1^{(k,i)} = D_1^{(k,i)} \cdot \theta_1^{(k,i)} \quad \hat{\theta}_2^{(k,i)} = D_2^{(k,i)} \cdot \theta_2^{(k,i)} \quad (10)$$

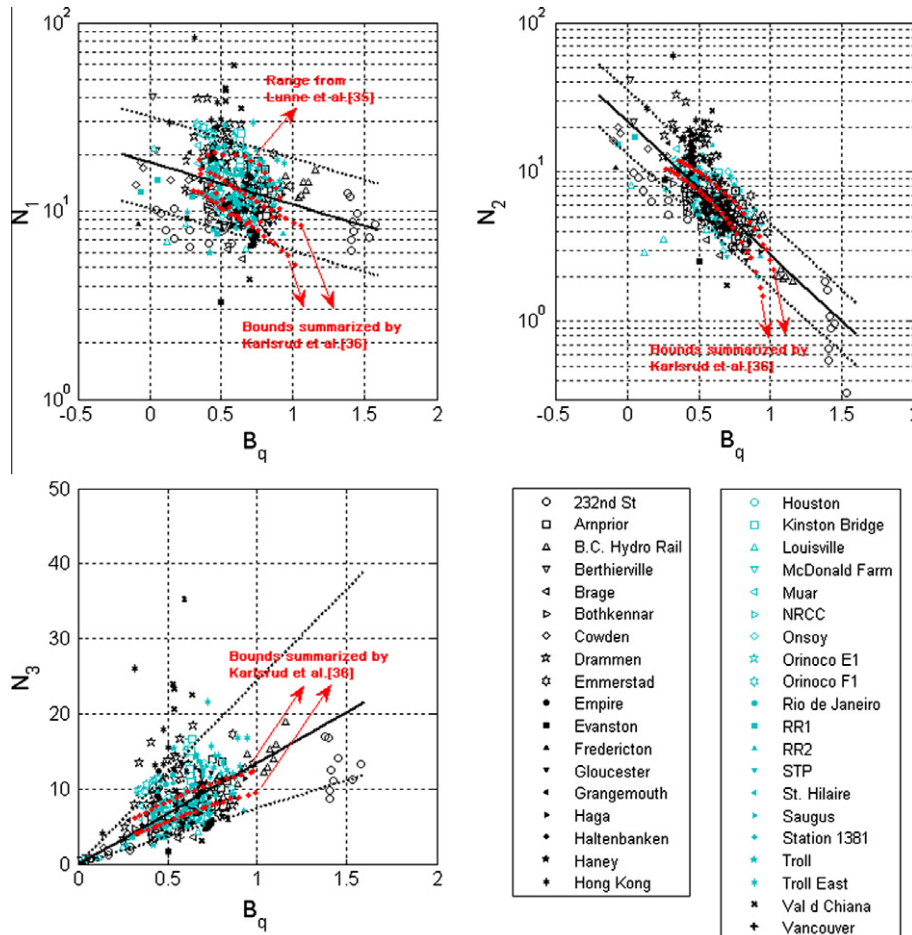


Fig. 2. Data points of all sites for the three models. Also shown are the generic trends (solid lines) and 95% confidence intervals (dashed lines) for the three correlation models and the ranges reported by Lunne et al. [35] and Karlsrud et al. [36].

where $D_1^{(k,i)}$ and $D_2^{(k,i)}$ are lognormally distributed with median value = 1 and c.o.v. = $\delta_1 = \delta_2 \approx 0.1$ [the estimation of the measurement errors in θ_3 is not necessary because θ_3 vanishes in (7)]; for the pore pressure ratio B_q

$$\widehat{B}_q^{(k,i)} = B_q^{(k,i)} + V_{Bq}^{(k,i)} \quad (11)$$

where $V_{Bq}^{(k,i)}$ is with zero mean value and standard deviation σ_{Bq} , estimated to be 0.1.

4.1. Quantification of the local transformation uncertainties

The data points in the global database are taken to quantify the “local” transformation uncertainties for each site. It is already seen in Fig. 1 that the local trends of the correlations are region-dependent or site-dependent. In this section, the focus is to estimate the magnitude of “local” transformation uncertainties, i.e. $E_{L,j}^{(k,i)}$ in (6). As illustrated in Fig. 3 for an N_2 -model data points in Hong Kong, the scatter around the local trend includes not only local transformation uncertainties but also measurement errors. In particular, the scatter reflects the variability of the term $\ln(\widehat{N}_2^{(k,i)}) - a_2^{(k)} - b_2^{(k)} \widehat{B}_q^{(k,i)}$ rather than the desired $\ln(N_2^{(k,i)}) - a_2^{(k)} - b_2^{(k)} B_q^{(k,i)}$, the former is contaminated by measurement errors.

In fact, the standard deviation of the total variability in $\ln(\widehat{N}_2^{(k,i)}) - a_2^{(k)} - b_2^{(k)} \widehat{B}_q^{(k,i)}$ should be in the order of

$$\sigma_{T,2}^{(k)} \approx \sqrt{\ln(1 + \delta_{Su}^2) + \ln(1 + \delta_2^2) + b_2^{(k)2} \sigma_{Bq}^2 + \sigma_2^{(k)2}} \quad (12)$$

where $\sigma_{T,2}^{(k)}$ denotes the standard deviation of the total scatter for the observed data points obtained in the k th site, and $\sigma_2^{(k)}$ denotes the standard deviation of the local transformation uncertainties for the k th site. It is then clear that $\sigma_{T,2}^{(k)} > \sigma_2^{(k)}$ – the magnitude of the local transformation uncertainties is less than the observed scatter. A plausible and simple way of estimating the standard deviation of local transformation uncertainties is as follows: given the data points for the k th site, first estimate $a_2^{(k)}$ and $b_2^{(k)}$ by least squares. The total standard deviation $\sigma_{T,2}^{(k)}$ can then be estimated as the sample standard deviation of the fitting errors. By using (12), the standard deviation $\sigma_2^{(k)}$ for the local transformation uncertainties can therefore be estimated as

$$\sigma_2^{(k)} \approx \sqrt{\sigma_{T,2}^{(k)2} - \ln(1 + \delta_{Su}^2) - \ln(1 + \delta_2^2) - b_2^{(k)2} \sigma_{Bq}^2} \quad (13)$$

The above steps can be similarly applied to estimate $\sigma_1^{(k)}$ and $\sigma_3^{(k)}$ for the N_1 and N_3 models.

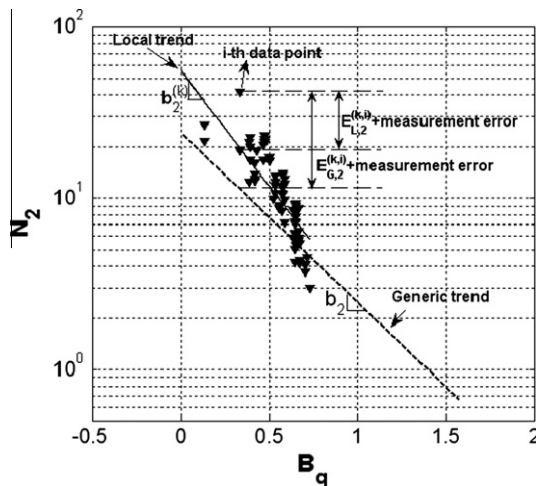


Fig. 3. Data points for the N_2 -model for the Hong Kong site.

The estimated local mean trends $a_j^{(k)} + b_j^{(k)} B_q$ are already shown in Fig. 1, while the estimated local transformation standard deviations $\sigma_j^{(k)}$ are not shown in the figure but are found to be usually quite small. There are even cases where the estimated $\sigma_j^{(k)}$ are close to zero – for those cases, it is likely that δ_{Su} , δ_j and σ_{Bq} are over-estimated. That is, $\sigma_j^{(k)}$ close to zero are most likely incorrect.

Judging from the relatively small standard deviations for the local transformation uncertainties, it is evident that the actual CPTU values are highly correlated to the actual value of S_u , at least in a local sense. However, the trends of the correlations are site dependent, so the correlation in one site may not be applicable to another site. It is quite likely that some factors other than q_T , u_2 and B_q are systematically affecting S_u ; in other words, S_u cannot be fully explained away by q_T , u_2 and B_q . These systematic “missing factors” will be captured as generic transformation uncertainties in the ensuing analysis.

5. Quantification of the generic transformation uncertainties

A conclusion from the previous section is that the CPTU– S_u correlation (mean trend) obtained at a site may not be applicable to another site, although the local transformation uncertainties are quite small. A sensible strategy is therefore to establish a “generic” CPTU– S_u correlation that is derived from the global database. A key hypothesis here is to treat the errors that cannot be fully explained away by q_T , u_2 and B_q as the “generic transformation uncertainties”. The generic transformation uncertainties are exactly $E_{G,j}^{(k,i)}$ as defined by (8). By doing so, the transformation uncertainties are now not separately treated within each site but are treated in a generic way.

Let all the generic transformation uncertainties $\{E_{G,j}^{(k,i)} : k = 1, \dots, n_s, i = 1, \dots, n_k\}$ (n_s is the total number of sites) be normally distributed with zero mean and standard deviation σ_j . Note that within a site, the generic transformation uncertainties $\{E_{G,j}^{(k,i)} : i = 1, \dots, n_k\}$ are not independent and are in fact highly correlated. The reason why this is the case is demonstrated in Fig. 3: the generic transformation errors for data points at the Hong Kong site $\{E_{G,j}^{(k,i)} : i = 1, \dots, n_k\}$ are mostly positive with respect to the generic trend line. For independent errors following a symmetric probability density function, the probability of say 20 errors being positive simultaneously is $0.5^{20} \approx 10^{-6}$ – practically impossible. Since the transformation errors that cannot be explained away by q_T , u_2 and B_q are usually systematic rather than random, the data points within a site may behave similarly and therefore share the same systematic error. However, the generic transformation uncertainties may be independent across sites. As a consequence, the covariance matrix of $\{E_{G,j}^{(k,i)} : k = 1, \dots, n_s, i = 1, \dots, n_k\}$ is block diagonal:

$$\Sigma_{E_j} = \begin{bmatrix} \overbrace{\begin{matrix} \sigma_j^2 & \cdots & \sigma_j^2 \\ \vdots & \ddots & \vdots \\ \sigma_j^2 & \cdots & \sigma_j^2 \end{matrix}}^{n_1 \text{ data points}} & & \\ & \ddots & \\ & & \overbrace{\begin{matrix} \sigma_j^2 & \sigma_j^2 & \cdots & \sigma_j^2 \\ \sigma_j^2 & \sigma_j^2 & & \sigma_j^2 \\ \vdots & & \ddots & \vdots \\ \sigma_j^2 & \sigma_j^2 & \cdots & \sigma_j^2 \end{matrix}}^{n_2 \text{ data points}} & & \\ & & & \ddots & \end{bmatrix} \quad (14)$$

Table 3
Characterization of generic transformation uncertainties.

N_1			N_2			N_3	
a_1	b_1	σ_1	a_2	b_2	σ_2	b_3	σ_3
2.896	−0.513	0.282	3.079	−2.049	0.243	13.442	0.298

Here it has been assumed that inter-site transformation uncertainties are independent, while intra-site ones are highly correlated. The use of the above matrix has the following desirable effect: the estimated parameters a_j , b_j , σ_j for the generic transformation will not be dominated by the sites with many data points (e.g. Hong Kong and McDonald's Farm).

A simple derivation shows that for the N_1 and N_2 models, the maximum likelihood estimate for a_j , b_j , σ_j ($j = 1$ or 2) are the ones that maximize the following log-likelihood function:

$$-1/2 \cdot \ln[\det(\Sigma_j)] - 1/2 \cdot [\ln(\hat{N}_j) - a_j \cdot \mathbf{1}_{n \times 1} - b_j \hat{B}_q]^T \Sigma_j^{-1} [\ln(\hat{N}_j) - a_j \cdot \mathbf{1}_{n \times 1} - b_j \hat{B}_q] \quad (15)$$

where

$$\Sigma_j = [\ln(1 + \delta_{Su}^2) + \ln(1 + \delta_j^2) + b_j^2 \sigma_{Bq}^2] \cdot I_{n \times n} + \Sigma_{E_j} \quad (16)$$

and

$$\begin{aligned} \hat{N}_j &= [\hat{N}_j^{(1,1)} \quad \dots \quad \hat{N}_j^{(1,n_1)} \quad \hat{N}_j^{(2,1)} \quad \dots \quad \hat{N}_j^{(2,n_2)} \quad \dots \quad \dots]^T \\ \hat{B}_q &= [\hat{B}_j^{(1,1)} \quad \dots \quad \hat{B}_j^{(1,n_1)} \quad \hat{B}_j^{(2,1)} \quad \dots \quad \hat{B}_j^{(2,n_2)} \quad \dots \quad \dots]^T \\ \mathbf{1}_{n \times 1} &= [1 \quad \dots \quad 1 \quad 1 \quad \dots \quad 1 \quad \dots \quad \dots]^T \end{aligned} \quad (17)$$

where n is the total number of data points and $I_{n \times n}$ is the identity matrix of size $(n \times n)$. For the N_3 model, the maximum likelihood estimate for b_3, σ_3 are the ones that maximize the following log-likelihood function:

$$-1/2 \cdot \ln[\det(\Sigma_3)] - 1/2 \cdot [\ln(\hat{\theta}_1) - \ln(a_3) \cdot \mathbf{1}_{n \times 1} - \ln(\hat{S}_u)]^T \Sigma_3^{-1} [\ln(\hat{\theta}_1) - \ln(a_3) \cdot \mathbf{1}_{n \times 1} - \ln(\hat{S}_u)] \quad (18)$$

where

$$\begin{aligned} \Sigma_3 &= [\ln(1 + \delta_{Su}^2) + \ln(1 + \delta_1^2)] \cdot I_{n \times n} + \Sigma_{E_3} \\ \hat{\theta}_1 &= [\hat{\theta}_j^{(1,1)} \quad \dots \quad \hat{\theta}_j^{(1,n_1)} \quad \hat{\theta}_j^{(2,1)} \quad \dots \quad \hat{\theta}_j^{(2,n_2)} \quad \dots \quad \dots]^T \\ \hat{S}_u &= [\hat{S}_u^{(1,1)} \quad \dots \quad \hat{S}_u^{(1,n_1)} \quad \hat{S}_u^{(2,1)} \quad \dots \quad \hat{S}_u^{(2,n_2)} \quad \dots \quad \dots]^T \end{aligned} \quad (19)$$

and Σ_{E_3} is defined similarly to (14).

The data points shown in Fig. 2 are taken to quantify the generic transformation uncertainties. It is of interest to address the following questions: (1) how do the generic trends differ from the local ones shown in Fig. 1? and (2) how do the generic standard deviations differ from the local ones? Table 3 summarizes the generic transformation uncertainties, including the a_j and b_j coefficients and the standard deviations of the generic transformation errors σ_j . Fig. 2 plots the generic trends (solid lines) as well as the 95% confidence intervals (dashed lines). The generic trends are more or less similar to the average of the local trends in Fig. 1. It is also evident that the standard deviations of the generic transformation uncertainties are significantly larger than those of local ones. The 95% confidence intervals for these generic correlation equations cover most local trends as well as the bounds/ranges proposed by the literature.

6. Recommended generic CPTU– S_u transformations

Based on the preceding sections, the generic transformation uncertainties seem much larger than local ones. A potentially con-

servative approach is therefore to apply the generic uncertainties. In the following, the derivations for the mean values and c.o.v. of S_u based on the generic CPTU– S_u transformations are derived. For the N_1 and N_2 models, S_u is correlated to CPTU data through the following equation:

$$\begin{aligned} \ln(S_u) &= \ln(\theta_j) - a_j - b_j B_q - E_{G,j} \\ &= \ln(\hat{\theta}_j) - a_j - b_j \hat{B}_q - \ln(D_j) + b_j V_{Bq} - E_{G,j} \end{aligned} \quad (20)$$

It is then clear that the mean value and standard deviation of $\ln(S_u)$ are

$$E[\ln(S_u)] = \ln(\hat{\theta}_j) - a_j - b_j \hat{B}_q \quad \text{std}[\ln(S_u)] \approx \sqrt{\ln(1 + \delta_j^2) + b_j^2 \sigma_{Bq}^2 + \sigma_j^2} \quad (21)$$

By using the closed-form relations between lognormal and Gaussian variables, it can be estimated that

$$\begin{aligned} E(S_u) &\approx \exp(E[\ln(S_u)] + 0.5 \text{std}[\ln(S_u)]^2) \\ &= \sqrt{1 + \delta_j^2} \cdot \hat{\theta}_j \cdot \exp(-a_j - b_j \hat{B}_q + 0.5 b_j^2 \sigma_{Bq}^2 + 0.5 \sigma_j^2) \\ \text{c.o.v.}(S_u) &\approx \sqrt{\exp(\text{std}[\ln(S_u)]^2) - 1} = \sqrt{(1 + \delta_j^2) \exp(b_j^2 \sigma_{Bq}^2 + \sigma_j^2) - 1} \end{aligned} \quad (22)$$

For the N_3 model, S_u is correlated to CPTU data through the following equation:

$$S_u = \frac{\theta_3}{b_3 B_q \cdot \exp(E_{G,3})} = \frac{\hat{\theta}_3}{b_3 D_1 \hat{B}_q \cdot \exp(E_{G,3})} \quad (23)$$

It follows that the mean value and c.o.v. S_u are

$$E(S_u) = \frac{\hat{\theta}_3}{b_3 \hat{B}_q} E\left(\frac{1}{D_1 \cdot \exp(E_{G,3})}\right) \quad \text{c.o.v.}(S_u) = \text{c.o.v.}\left(\frac{1}{D_1 \cdot \exp(E_{G,3})}\right) \quad (24)$$

By using the closed-form relations between lognormal and Gaussian variables, it can be estimated that

$$E(S_u) \approx \frac{\sqrt{1 + \delta_1^2} \cdot \hat{\theta}_3 \cdot \exp(0.5 \sigma_3^2)}{b_3 \hat{B}_q} \quad \text{c.o.v.}(S_u) \approx \sqrt{(1 + \delta_1^2) \exp(\sigma_3^2) - 1} \quad (25)$$

Table 4 summarizes the mean values and c.o.v.s of the S_u estimates based on the three generic transformation models. Note that the estimated S_u is the CIUC-reference undrained shear strength. For S_u from other test types, proper transformations must be further applied (e.g. [42–44]). Based on the magnitudes of the c.o.v.s, it is clear that the three generic models give comparable transformation uncertainty.

It is advised that when local CPTU– S_u trend is known from site investigation, the design S_u can be estimated from CPTU data based on the local trend, while the c.o.v. of the generic transformation in Table 4 can be adopted for conservatism. When the local CPTU– S_u trend is not known, the generic mean in Table 4 can be used to estimate the design S_u CPTU data, and the generic c.o.v. in Table 4 can be adopted.

Table 4
Generic mean values and c.o.v.s of the S_u estimates for three models.

Model	$E(S_u)$	c.o.v. (S_u)
N_1	$0.0578 \cdot (\hat{q}_T - \hat{\sigma}_{\sigma 0}) \cdot \exp(0.513 \hat{B}_q)$	0.31
N_2	$0.0486 \cdot (\hat{q}_T - \hat{u}_2) \cdot \exp(2.049 \hat{B}_q)$	0.34
N_3	$0.0782 \cdot (\hat{u}_2 - \hat{u}_0) / \hat{B}_q$	0.32

7. Verification of generic transformations

Based on the local and generic analysis results, there seems to be an apparent contradiction: for a single site with few boreholes and data points, the standard deviation of transformation uncertainties is quite small, while for the generic case with many sites, the standard deviation is significantly larger. It is natural to question if the so-called “generic” estimates listed in Table 4 are indeed more generic than those derived from single sites? It is therefore of interest (a) to understand the prediction performance of these equations and (b) to assess if 38 sites in the global database are enough to provide generic mean and generic c.o.v. estimates.

Regarding Question (a), validation database (see Table 5) from 11 sites in two countries, Singapore and Sweden, is taken to examine the applicability of the important statistical guidelines given in Table 4. There are 290 data points in total in the validation database. These datasets are not included in the global database described in Table 1. In fact, there are no Singapore and Sweden data points in Table 1. All undrained shear strengths for the validation database were also converted to their CIUC-equivalent values for consistency.

The verification is conducted in Fig. 4, in a manner similar to Fig. 2: the markers show the measured N factors (vertical axis) and measured B_q values (horizontal axis) for the data points in the validation database, while the solid lines and confidence intervals are based on the statistical guidelines recommended in Table 4. For Sweden data points, the scattering is less, and most data points are close to the central generic trend lines. The equations and c.o.v.s in Table 4 over-predict the uncertainties. However, this is not surprising at all because those equations and c.o.v.s are meant to be generic – it is likely to overestimate local transformation uncertainties.

For the Singapore dataset, there are nearly 200 validation data points, showing a larger scatter. This may be because the Singapore data are provided by commercial companies. It is expected to exhibit a larger scatter compared to data from research studies. Yet it is reassuring to observe that most of the data points fall within the confidence intervals. The equations and c.o.v.s in Table 4 satisfactorily predict the uncertainties in these data points. Notice that there are only two Asian sites (Hong Kong and Malaysia) in the database described in Table 1, and yet the resulting 95% confidence interval can still cover the Singapore data points quite well. The statistical guidelines given in Table 4 appear to be quite robust and are potentially useful for reliability calibration in the absence

of local statistical data. They are also useful as prior information in Bayesian updating, even if local data are available.

To address Question (b), it is of interest to see how the prediction performance varies as the number of calibration sites increases. Recall that there are 38 sites in the global database. If the equations based on some smaller subsets of the global database (number of sites much less than 38) always perform similarly to those in Table 4, the latter equations should be already sufficiently generic, i.e. adding more sites to the global database should not significantly change these equations. Therefore, these equations can be used in a robust way for reliability-based design in the absence of site specific information. On contrary, if the equations based on a comparable database (number of sites close to 38) perform quite differently from the equations in Table 4, the latter equations may not be sufficiently generic, i.e. adding more sites should significantly change these equations.

Question (b) is studied using a bootstrap strategy consisting of drawing random subsets from the global database. To provide a concrete illustration of this random draw, we restrict our attention to the estimation of the so-called cross-validation (CV) error rate (defined below) based on data from n sites. Random subsets containing n sites can be drawn from the global database containing 38 sites as follows:

1. Draw site #1 randomly (equal probability) from 38 sites.
2. Draw site #2 randomly from remaining 37 sites.
3. ...
4. Draw site # n randomly from remaining $38 - n + 1$ sites.
5. Record the number of data points in site#1, site#2, ..., site# n .
6. Repeat the procedure 10 times to get 10 subsets.

To let the 10 subsets be reasonably distinct, n is restricted to be less than 30. This ensures that there are a large number of distinct subsets and that the chance of repeating the same subset within the 10 draws is small.

From each data subset, the model parameters and standard deviation $\{a_i, b_i, \sigma_i\}$ are estimated and the 95% confidence intervals are found. Then, the validation database (Singapore and Sweden data points) is applied, and the CV error rate is defined to be the percentage of the validation data points that are outside the 95% confidence interval. Doing so for 10 subsets will yield useful plots that show the variation of the CV error rates with respect to the numbers of sites or alternately, the number of data points. An example of these plots is given in Fig. 5 for the validation of N_1 model, which clearly

Table 5
Basic information of the validation database.

k	Site	Region	Clay description (range of sensitivity if available)	# Points with S_u	Area ratio	Filter location	S_u Test type					Atterberg limits	OCR	References
							UC	UU	CIUC	CAUC	VST			
1	Gota Alv	Gothenburg (Sweden)	Marine post-glacial clay	11	–	u_2					*	*	*	[48]
2	Munkedal	Gothenburg (Sweden)	Quick clay	11		u_2					*		*	[48]
3	Norfolk Road	Singapore	Marine clay	14	–	u_1		*			*	*	*	[23]
4	Norrköping	Norrköping (Sweden)	Grey varved clay/thin silt layer	32	–	u_2					*	*	*	[48]
5	Singapore 1	Singapore	LOC Silty marine (3–4)	20	0.8	u_2		*			*	–	*	[49]
6	Singapore 2	Singapore	LOC Silty marine (3–4)	18	0.8	u_2		*			*	–	*	[49]
7	Singapore 3	Singapore	LOC Silty marine (3–4)	7	0.8	u_2		*			*	–	*	[49]
8	Singapore kJ_BH	Singapore	LOC Silty marine (3–4)	139	0.8	u_2		*			*	–	*	[49]
9	Svartioland	Stockholm (Sweden)	Soft Clay	16	–	u_2					*	*	*	[48]
10	Stora an	Gothenburg (Sweden)	Green-gray clay	7	–	u_2					*	*	*	[48]
11	Upplands-Vasby	Stockholm (Sweden)	Clay	15		u_2					*	*	*	[50,51]

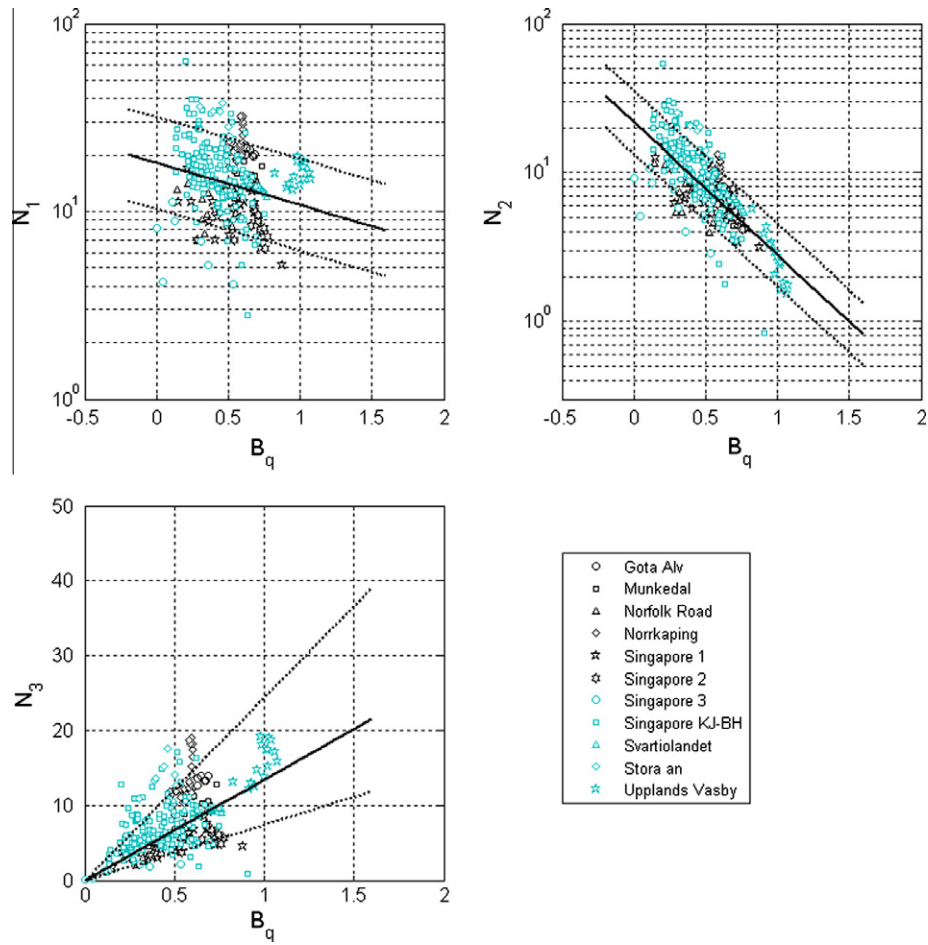


Fig. 4. Verification results using Singapore and Sweden database over the three correlation models.

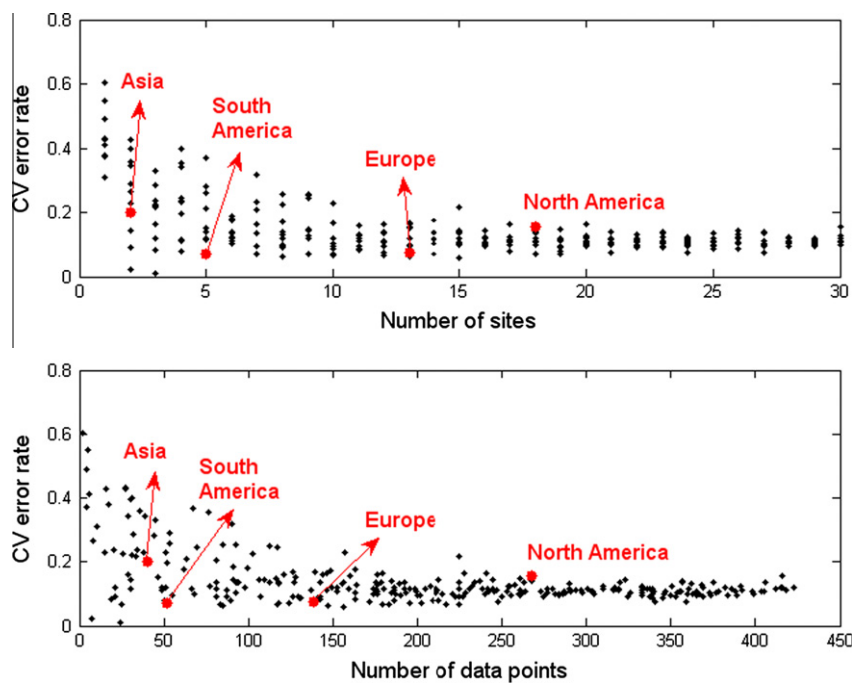


Fig. 5. Variation of CV error rates with respect to the numbers of sites (top) and data points (bottom) for the N_1 model.

indicate that the CV error rates can be unstable when the number of sites or data points is small. Although not shown, the validation plots for N_2 and N_3 models show similar results.

From Fig. 5, it can be seen that signs of convergence first appear at about 10 sites or 150 data points. For smaller sample sizes, the CV error rates fluctuate erratically. In other words, it is possible to realize a low CV error rate by “luck”, but it is not possible to do so consistently if there are only less than about 10 sites. The estimates are close to the final values when the number of sites is more than 15 or when the number of data points is more than 250. Note that the entire database consists of 38 sites and 482 data points, which are significantly larger than the threshold numbers – 15 sites and 250 data points. The practical conclusion here is that the estimates reported in Table 4 may be stable and reliable as “generic” estimates. Fig. 5 also shows the CV error rates for some regions, including Asia, North America, South America and Europe. The results show that as long as the number of sites or the number of data points is large enough with the accompanying implicit assumption that sufficient geographical coverage typically implies sufficient geologic diversity (e.g. North America – 18 sites), the CV error rates for the regional estimates can be quite close to the CV error rates based on all 38 sites. On the contrary, if the number of sites or the number of data points is not enough (e.g. Asia – 2 sites), the CV error rates for the regional estimates can be quite different from the generic ones based on 38 sites. Although not shown, the conclusions for the N_2 and N_3 models are similar.

8. Conclusion

A study has been undertaken to characterize generic transformation uncertainties for geotechnical design parameters, exemplified by CPTU– S_u transformations. It is concluded that many of previous studies may only provide local trends for the CPTU– S_u transformations, i.e. results are site-specific. Analyses of a global database (38 sites, 482 data points) show that the magnitude of uncertainties is somewhat larger than those mentioned in the previous studies. The study further shows that a database of 15 sites may be sufficient to develop stable generic estimates of the CPTU– S_u transformation uncertainties.

Simple equations for three popular CPTU– S_u transformation models are developed based on the global database. Based on CPTU data, these equations are able to provide the mean S_u estimates as well as their coefficients of variation (c.o.v.), which are found to fall within a narrow range around 0.31–0.34. These transformation equations are examined using validation database from 11 sites in Singapore and Sweden. The verification exercise shows that the equations potentially are able to provide consistent mean and c.o.v. estimates of S_u in the absence of local data.

Because there are virtually no highly over consolidated and fissured clays in the database, the conclusion of this study may not be applicable to those clays. The quality of data is likely to be non-uniform given the varied sources. In spite of this limitation which is inevitable in a study of this nature, the significant size of the database and the relatively low estimated c.o.v. of 0.3 do indicate that the mean equations can be used with some degree of confidence. The transformation uncertainties estimated in this study are also likely to be representative of practical design scenarios than well-controlled research scenarios. In other words, they are probably upper bound values and can be applied to practical reliability-based design in the absence of local soil statistics.

References

- [1] Kulhawy FH. On evaluation of static soil properties. In: Seed RB, Boulanger RW, editors. *Stability and performance of slopes and embankments II* (GSP 31). New York: ASCE; 1992. p. 95–115.
- [2] Phoon KK. Reliability-based design of foundations for transmission line structures. Ph.D. Dissertation, Ithaca (NY): Cornell University; 1995.
- [3] Hara A, Ohta T, Niwa M, Tanaka S, Banno T. Shear modulus and shear strength of cohesive soils. *Soils Found* 1974;14(3):1–12.
- [4] Aas G, Lacasse S, Lunne T, Hoeg K. Use of in-situ tests for foundation design on clay. In: Clemence SP, editor. *Use of in-situ tests in geotechnical engineering* (GSP6), 1986. p. 1–30.
- [5] Robertson PK, Campanella RG, Gillespie D, Greig J. Use of piezometer cone data. *Use of in situ tests in geotechnical engineering* (GSP 6) 1986;1263–80.
- [6] Konrad JM, Law KT. Undrained shear strength from piezocone tests. *Can Geotech J* 1987;24(3):392–405.
- [7] Senneset K, Sandven R, Janbu N. Evaluation of soil parameters from piezocone tests. *Transportation research record no. 1235, in situ testing of soil properties for transportation*, 1989; p. 24–37.
- [8] Jamiolkowski M, Lancellotta R, Tordella L, Battaglio M. Undrained strength from CPT. In: *Proc. of the 2nd European symposium on penetration testing*, 1982. p. 599–606.
- [9] Lacasse S, Lunne T. Penetration tests in two Norwegian clays. In: *Proc. of the 2nd European symposium on penetration testing*. Amsterdam; 1982. p. 661–9.
- [10] Koutsoftas DC, Foot R, Handfelt LD. Geotechnical investigations offshore Hong Kong. *J Geotech Eng* 1987;113(2):87–105.
- [11] Rad NS, Lunne T. Direct correlations between piezocone test results and undrained shear strength of clay. In: *Proc. of the 1st international symposium on penetration testing, ISOPT-1, Orlando*; vol. 2, 1988. p. 911–7.
- [12] Campanella RG, Sully JP, Robertson PK. Interpretation of piezocone soundings in clay – a case history. In: *Penetration testing in the UK*, Thomas Telford; 1988. p. 203–8.
- [13] Greig JW, Campanella RG, Robertson PK. Comparison of field vane results with other in-situ test results. In: *Soil mechanics series 106*, Vancouver: University of British Columbia; 1987. p. 247–263.
- [14] Konrad JM, Law KT. Preconsolidation pressure from piezocone tests in marine clays. *Geotechnique* 1987;37(2):177–90.
- [15] Rochelle PL, Zebdi M, Leroueil S, Tavenas F, Virely D. Piezocone tests in sensitive clays of eastern Canada. In: *Proc. of the 1st international symposium on penetration testing, ISOPT-1, Orlando*; vol. 2, 1988. p. 831–41.
- [16] Azzouz AS, Lutz DG. Shaft behavior of a model pile in plastic empire clays. *J Geotech Eng* 1986;112(4):389–406.
- [17] Fimmo RJ. Subsurface conditions and pile installation data: 1989 foundation engineering congress test section. In: Finno RJ, editor. *Predicted and observed axial behavior of piles* (GSP 23). New York; 1989. p. 1–14.
- [18] Valsangar AJ, Landva AO, Alkins JC. Performance of a raft foundation supporting a multi-storey building. In: *Proc. of 38th Canadian geotechnical conference*, Edmonton; 1985. p. 315–23.
- [19] Powell JMM, Quarterman RST. The interpretation of cone penetration tests in clays, with particular reference to rate effects. In: *Proc. of the 1st international symposium on penetration testing, ISOPT-1, Orlando*; vol. 2, 1988. p. 903–9.
- [20] Powell JMM, Uglov IM. Dilatometer testing in stiff overconsolidated clays. In: *Proc. of 39th Canadian geotechnical conference*, Ottawa; 1988. p. 317–26.
- [21] Mahar LJ, O'Neill MW. Geotechnical characterization of desiccated clay. *J Geotech Eng* 1983;109(1):56–71.
- [22] Long MM, O'Riordan NJ. The use of piezocone in the design of a deep basement in London clay. Thomas Telford (London): *Penetration Testing in the UK*; 1988. p. 173–6.
- [23] Chang MF. Interpretation of over consolidated ratio from in situ tests in recent clay deposits in Singapore and Malaysia. *Can Geotech J* 1991;28(2): 210–25.
- [24] Eden WJ, Law KT. Comparison of undrained shear strength results obtained by different test methods in soft clays. *Can Geotech J* 1980;17(3): 369–81.
- [25] Azzouz A, Baligh MM, Ladd CC. Cone penetration and engineering properties of soft Orinoco clay. In: *Proceedings, 3th international conference on behavior of offshore structure*, Cambridge, Massachusetts; vol. 1, 1983. p. 161–80.
- [26] Ramalho-Ortigao JA, Werneck MLG, Lacerda WA. Embankment failure on clay near Rio De Janeiro. *J Geotech Eng* 1983;109(11):1460–79.
- [27] Rocha-Filho P, Alencar JA. Piezocone tests in the Rio De Janeiro soft clay deposit. In: *Proc. of 11th international conference on soil mechanics and foundation engineering*, San Francisco; vol. 2, 1985. p. 859–862.
- [28] Sills GC, Almeida MSS, Danziger FAB. Coefficient of consolidation from piezocone dissipation tests in a very soft clay. In: *Proc. of 1st international symposium on penetration testing, Orlando*; vol. 2, 1988. p. 967–74.
- [29] Coutinho RQ. Characterization and engineering properties of Recife soft clays – Brazil. In: *Proc. of the international workshop on characterisation and engineering properties of natural soil*, Singapore; 2007. p. 2049–99.
- [30] Lafleur J, Silvestri V, Asselin R, Soulie M. Behavior of a test excavation in soft Champlain sea clay. *Can Geotech J* 1988;25(4):705–15.
- [31] Baligh MM, Vivatrat V, Ladd CC. Cone penetration in soil profiling. *J Geotech Eng, ASCE* 1980;106(4):447–61.
- [32] Amundsen T, Lunne T, Christophersen HP, Bayne JM, Barnwell CL. Advanced deep-water soil investigation at the Troll East field. In: *Proc. of advances in underwater technology*, London; vol. 2, 1985. p. 1–22.
- [33] Cancelli A, Cividini A. An embankment on soft clays with sand drains: numerical characterization of the parameters from in-situ measurements. In: *Proc. of international conference on case histories in geotechnical engineering*; 1984. p. 637–43.
- [34] Ching J, Phoon KK, Chen YC. Reducing shear strength uncertainties in clays by multivariate correlations. *Can Geotech J* 2010;47(1):16–33.

- [35] Lunne T, Christophersen HP, Tjelta TI. Engineering use of piezocone data in North Sea clays. In: International conference on soil mechanics and foundation engineering 11, San Francisco; vol. 2, 1985. p. 907–12.
- [36] Karlsrud K, Lunne T, Brattlien K. Improved CPTU interpretations based on block samples. *Norw Geotech Inst, Oslo* 1997;202:195–201.
- [37] Kulhawy FH, Birgisson B, Grigoriu MD. Reliability-based foundation design for transmission line structures: transformation models for in-situ tests. Report EL-5507(4), Palo Alto: Electric Power Research Institute; 1992.
- [38] Chen BS-Y. Profiling stress history of clays using dual element piezocones. Ph.D. Dissertation, Georgia Institute of Technology; 1994.
- [39] Hight DW, Bond AJ, Legge JD. Characterization of the Bothkennar clay: an overview. *Geotechnique* 1992;42(2):303–47.
- [40] Phoon KK. Reliability-based design of foundations for transmission line structures, Report EL-5507, EPRI; January 1992.
- [41] Lunne T, Robertson PK, Powell JJM. Cone penetrating testing: in geotechnical practice. Chapman & Hall; 1997.
- [42] Mayne PW, Kulhawy FW, Kay JN. Observations on the development of pore-water stresses during piezocone penetration in clays. *Can Geotech J* 1990;27(3):418–28.
- [43] Kulhawy FH, Mayne PW. Manual on estimating soil properties for foundation design, Report EL6800, EPRI; August 1990.
- [44] Chen YJ, Kulhawy FH. Undrained strength interrelationships among CIUC, UU, and UC tests. *J Geotech Eng* 1993;119(11):1732–50.
- [45] Bjerrum L. Embankment on soft ground. In: Proceedings of ASCE specialty conference on performance of earth and earth-supported structures, Lafayette; 1972.
- [46] Akaike H. A new look at the statistical model identification. *IEEE Trans Autom Control* 1974;AC-19:716–23.
- [47] Schwarz G. Estimating the dimension of a model. *Ann Stat* 1978;6:461–4.
- [48] Larsson R, Mulabdic M. Piezocone tests in clay. Swedish geotechnical institute report, 42, Linkoping, Sweden; 1991. p. 240.
- [49] Chang MF. Some experience with the dilatometer test in Singapore. In: Proc. of 1st international symposium on penetration testing, Orlando; vol. 1, 1988. p. 489–96.
- [50] Battaglio M, Jamiolkowski M. Interpretation of CPT's and CPTU's proceedings. In: Fourth international geotechnical seminar: field instrumentation and in-situ measurements, Singapore; 1986. p. 129–43.
- [51] Bayne JM, Tjelta TI. Advanced cone penetrometer development for in-situ testing at Gullfaks C. In: Proceedings, 19th offshore technology conference, Houston; vol. 4, 1987. p. 531–40.